

APPLICATION OF IMAGE ANALYSIS TO IMPROVE OBJECT IDENTIFICATION AND INVENTORY
ASSESSMENT BY UAS

by

PRADEEP KUMAR RAGU CHANTHAR

(Under the direction of Chris Cieszewski)

ABSTRACT

This project discusses the Geographic information system (GIS) analysis in calculating the woody debris volume in post harvest forest sites in B.F. Grant Forest. The estimation of the biomass volume of timber residues by traditional methods is time consuming and expensive. An unmanned aerial system (UAS) mounted with a small camera captures the images of four different plots in the B.F Grant Forest. A 3D model of each plot was developed using aerial images captured by the UAS camera. A new methodology for the calculation of the biomass volume from a 3D shape model of the woody debris is introduced in this project. It involves the development of two models: DEM (digital elevation model) and DSM (digital surface model). To validate the calculation, the wood was collected manually from the plots and the biomass volume of timber residues was calculated using line intersect sampling method.

INDEX WORDS: UAS, Line intersect, Structure from motion, Geographic information system and biomass

APPLICATION OF IMAGE ANALYSIS TO IMPROVE OBJECT IDENTIFICATION AND INVENTORY
ASSESSMENT BY UAS

by

PRADEEP KUMAR RAGU CHANTHAR

B.Tech., Anna University, 2011

A Thesis Submitted to the Graduate Faculty
of The University of Georgia in Partial Fulfillment
of the
Requirements for the Degree

MASTER OF SCIENCE

ATHENS, GEORGIA

2015

© 2015

Pradeep Kumar Ragu Chanthar

All Rights Reserved

APPLICATION OF IMAGE ANALYSIS TO IMPROVE OBJECT IDENTIFICATION AND INVENTORY
ASSESSMENT BY UAS

by

PRADEEP KUMAR RAGU CHANTHAR

Approved:

Major Professor: Chris Cieszewski

Committee: Pete Bettinger
Marguerite Madden

Electronic Version Approved:

Suzanne Barbour
Dean of the Graduate School
The University of Georgia
December 2015

DEDICATION

To my parents

&

late former President of India Dr. Abdul Kalam.

ACKNOWLEDGEMENTS

I would like to thank my major professor Dr. Chris Cieszewski for guiding me throughout my masters. He is patient and supportive, and has always helped me to understand the study and scientific writings. Thank you for educating me.

I would like to thank Dr. Pete Bettinger for his support & feedback. He has helped me to understand forest planning. Thank you for offering me the U.S. Forest service internship position.

I would like to thank Dr. Marguerite Madden for her mentorship and for accepting me to be part of CGR(Center for Geospatial Research). I have learnt remote sensing, photogrammetry and aerial photography because of her. Without her, I would not have learnt GIS.

Thank you Dr. Larry Morris for offering me this wonderful project. I would like to extend my gratitude to Ogden and Chris Warren for helping me in the field data collection.

Special thanks to Dr. Tommy Jordon. He is the one who guided me throughout my thesis project and helped me in UAS field data collection, and in discovering the new algorithm for my thesis project.

Finally, I would like to thank Roshini Ramachandran for supporting me in all the ways that she could and all my friends for their support.

TABLE OF CONTENTS

| | Page |
|--|------|
| ACKNOWLEDGEMENTS | v |
| LIST OF FIGURES | viii |
| LIST OF TABLES | x |
| CHAPTER | |
| 1 INTRODUCTION, RESEARCH OBJECTIVES AND STUDY AREA | 1 |
| 1.1 INTRODUCTION | 1 |
| 1.2 RESEARCH OBJECTIVES | 2 |
| 1.3 STUDY AREA | 3 |
| 1.4 THESIS STRUCTURE | 3 |
| 2 LITERATURE REVIEW | 7 |
| 2.1 USE OF LIDAR IN ESTIMATING VOLUME OF BIOMASS OF COARSE WOODY DEBRIS | 8 |
| 2.2 STRUCTURE FROM MOTION | 12 |
| 3 MATERIALS AND METHODS | 13 |
| 3.1 FIRST TEST SITES | 13 |
| 3.2 SECOND TEST SITE | 13 |
| 3.3 UAS FLIGHTS | 14 |
| 3.4 FIELD ESTIMATES OF CWD VOLUME | 15 |
| 3.5 AERIAL ESTIMATIONS OF CWD VOLUME | 17 |
| 3.6 DIGITAL ELEVATION MODEL | 20 |

| | | |
|-----|---|----|
| 3.7 | DIGITAL SURFACE MODEL | 21 |
| 3.8 | DIFFERENCE OF DEM AND DSM OF PLOT 1 | 21 |
| 4 | RESULTS AND DISCUSSION | 24 |
| 4.1 | WOODY DEBRIS VOLUME ESTIMATION | 24 |
| 4.2 | TEST SITE 2 RESULTS | 27 |
| 5 | CONCLUSIONS | 30 |
| | BIBLIOGRAPHY | 31 |

LIST OF FIGURES

| | | |
|-----|---|----|
| 1.1 | Test plot: Three-dimensional point cloud image of the woody residue remaining on a recently harvested forest site. This model is generated using the images extracted from the video taken by the small camera of the UAS and georeferenced using the five targets set up in the field. | 2 |
| 1.2 | Map of the B.F. Grant Forest, (Source: D. B. Warnell School of Forestry and Natural Resources, University of Georgia, Athens, GA. Unpublished) | 5 |
| 1.3 | 2014 Timber sale map-B.F. Grant Forest, (Source: D. B. Warnell School of Forestry and Natural Resources, University of Georgia, Athens, GA. Unpublished) | 6 |
| 2.1 | Flight path to capture vertical aerial photograph [5] | 11 |
| 2.2 | Input images used to construct 3D model- structure from motion [25] | 12 |
| 3.1 | Location of plots and transects within each of four 0.25 ha plots at the B.F. Grant Forest, Source: Chris Warren, D. B. Warnell School of Forestry and Natural Resources, University of Georgia, Athens, GA. | 14 |
| 3.2 | Location of plots and transects within each of four 0.25 ha plots at the B.F. Grant Forest, Source: Chris Warren, D. B. Warnell School of Forestry and Natural Resources, University of Georgia, Athens, GA. | 15 |
| 3.3 | Aerial view of Test Site 2 containing ground control points and target of known volume in Whitehall Forest. | 16 |
| 3.4 | Unmanned Aerial System(UAS)(DJI Phantom 2 Vision Plus quadcopter) | 17 |
| 3.5 | Example of a standard flight path flown by the quadcopter to capture video images of 50 m x 50 m plots | 18 |
| 3.6 | Overview of steps used for aerial estimation of woody biomass volume. | 19 |

| | | |
|------|---|----|
| 3.7 | 3D model of Plot 1 created using Photoscan. (Blue flags represent the image angles and images used to developed the 3D model). | 19 |
| 3.8 | Overview of the volume calculation algorithm | 20 |
| 3.9 | Digital Elevation Model of Plot 1 | 21 |
| 3.10 | Digital Surface Model of Plot 1 | 22 |
| 3.11 | Difference of DEM and DSM of Plot 1 | 23 |
| 3.12 | Sub plots of Plot 1 | 23 |
| 4.1 | 3D image with residue piles identified. Volumes associated with these piles were not included in either mini plot or line intersect sampling. They are appear to be responsible for differences in volume estimates between field sampling and 3D image sampling. | 27 |
| 4.2 | Removal of dead trees and bushes | 28 |

LIST OF TABLES

| | | |
|-----|--|----|
| 4.1 | Plot 1 off the Godfrey Road | 25 |
| 4.2 | Plot 2 off the Godfrey Road | 25 |
| 4.3 | Plot 3 along Indian Trail Road | 25 |
| 4.4 | Plot 4 along Indian Trail Road | 26 |
| 4.5 | Comparison of the manual and 3D image volume calculation of known target field in (m ³) | 29 |

CHAPTER 1

INTRODUCTION, RESEARCH OBJECTIVES AND STUDY AREA

1.1 INTRODUCTION

This project is focused on calculating the volume of woody debris from post-harvest sites of B.F. Grant Forest. The B.F. Grant Forest comprises of 4957.399 hectares. Line intersect sampling is one of various traditional methods to calculate the volume of woody debris, an essential component in terrestrial ecosystems. Woody debris refers to a collection of dead trees, logs, large branches, snags and chunks of wood in different sizes. Coarse woody debris is an essential component in the forest ecosystem which plays an important role in plant habitat and wildlife habitat.

Currently, there is a growing need to develop fast, reliable and inexpensive methods for estimating post-harvest woody biomass for the purposes of estimating and marketing biomass fuel, as well as to comply with state and certification organization biomass harvesting guidelines (BHG). Biomass fuel is a renewable energy useful for commercial and industry purposes. One possible approach to re-mediate issues being currently faced in quantifying biomass is the utilization of a low-cost and lightweight unmanned aerial system (UAS). This UAS is equipped with a video camera to provide high-resolution images (Figure 1.1), which can be subsequently analyzed by photogrammetry to provide us information in the form of 3D point clouds from which the woody debris volume can be estimated.

To test the utility of using image analyses, photogrammetry and 3D point clouds to estimate post-harvest coarse woody debris (CWD), plots were established on recently harvested loblolly pine and mixed-pine hardwood stands on the B.F. Grant Forest near Eatonton, GA in southeastern United States. At each plot, on-the-ground CWD volume was measured using traditional line intersect (or intercept) sampling of all debris greater than 4 cm in diameter along 50 m transects and by

woody debris piece measurement within 10 m x 10 m mini-plots randomly located within each of the larger plots. Results from this field sampling are compared with results from 3D point clouds derived from images acquired by a UAS (DJI Phantom 2 Vision Plus quadcopter) flown at 25-30 m height over these plots. Several post processing methods to estimate woody debris volumes calculated from the UAS imagery were tested. Ultimately, these estimates were compared with volume estimates from on-the-ground sampling.



Figure 1.1: Test plot: Three-dimensional point cloud image of the woody residue remaining on a recently harvested forest site. This model is generated using the images extracted from the video taken by the small camera of the UAS and georeferenced using the five targets set up in the field.

1.2 RESEARCH OBJECTIVES

The objective of this project was to estimate biomass volume from visual images of the woody debris from post-harvest sites recorded using a UAS survey, and to validate the photogrammetric measurements of biomass with the conventional methods of line-intercept and on-site plot biomass measurements which are currently being used for the estimation of post-harvest woody residues for pine and mixed pine-hardwood clearcut forests of the US Southeast region.

1.3 STUDY AREA

Four different 50 m square plots located in the B.F. Grant Forest (Eatonton, Georgia, United States of America, co-ordinates Latitude: $33^{\circ} 22' 39.35^{11}$ N, Longitude: $83^{\circ} 28' 17.33^{11}$ W) were used for the biomass estimation aspect of this thesis (Figure 1.2). Sites were selected after the post-harvest of timber and using maps of timber sale tracts (Figure 1.3), Google Earth and site visits.

After clearcut harvest, two plots (Site1, Site2), situated in Indian Creek Road and two plots (Site3, Site4), situated in Godfrey Road, were suitable for flying a UAS and taking aerial images for the biomass estimation since the sites were free of trees. The biomass of two mini plots on each site (10 m x 10 m) was estimated by a traditional method (line intersect sampling method) in order to validate the new methodology developed for UAS imagery. A 3D point cloud model of each site was developed, from which digital elevation and digital surface models (DEM and DSM, respectively) were developed to calculate the volume of the biomass. A 3D point cloud is a collection of points with x,y and z coordinates of high density (points are typically on the order of centimeters to millimeters apart) that together create 3D shapes of objects and landscape.

Additionally, to test the capability of the method proposed in this project, a small experiment is conducted in the Whitehall Forest, Athens, Georgia. Here, the experiment was conducted to compare volume calculated from UAS imagery to that of the known target. In this case the target was four paper boxes placed in the field of Whitehall Forest. Paper boxes dimensions were 72 inches in length, 11.5 inches in width and 9 inches in height.

1.4 THESIS STRUCTURE

The thesis structure is organized into five chapters. Chapter 1 explains the research objectives, and explains the study area. Chapter 2 reviews various methods of volume estimation of coarse woody debris. Traditional and recent methods were discussed. Chapter 3 explains the development of a method using system (UAS) unmanned aerial vehicle mounted with a small camera to capture aerial imagery and photogrammetry for the estimation of coarse woody debris following forest

harvesting. Furthermore it describes the relation between the manual traditional method and digital method for the calculation of biomass volume of the woody debris. Chapter 4 explains the results of both the manual calculation and UAS method proposed in this project. Chapter 5 summarizes the thesis and states important conclusions.

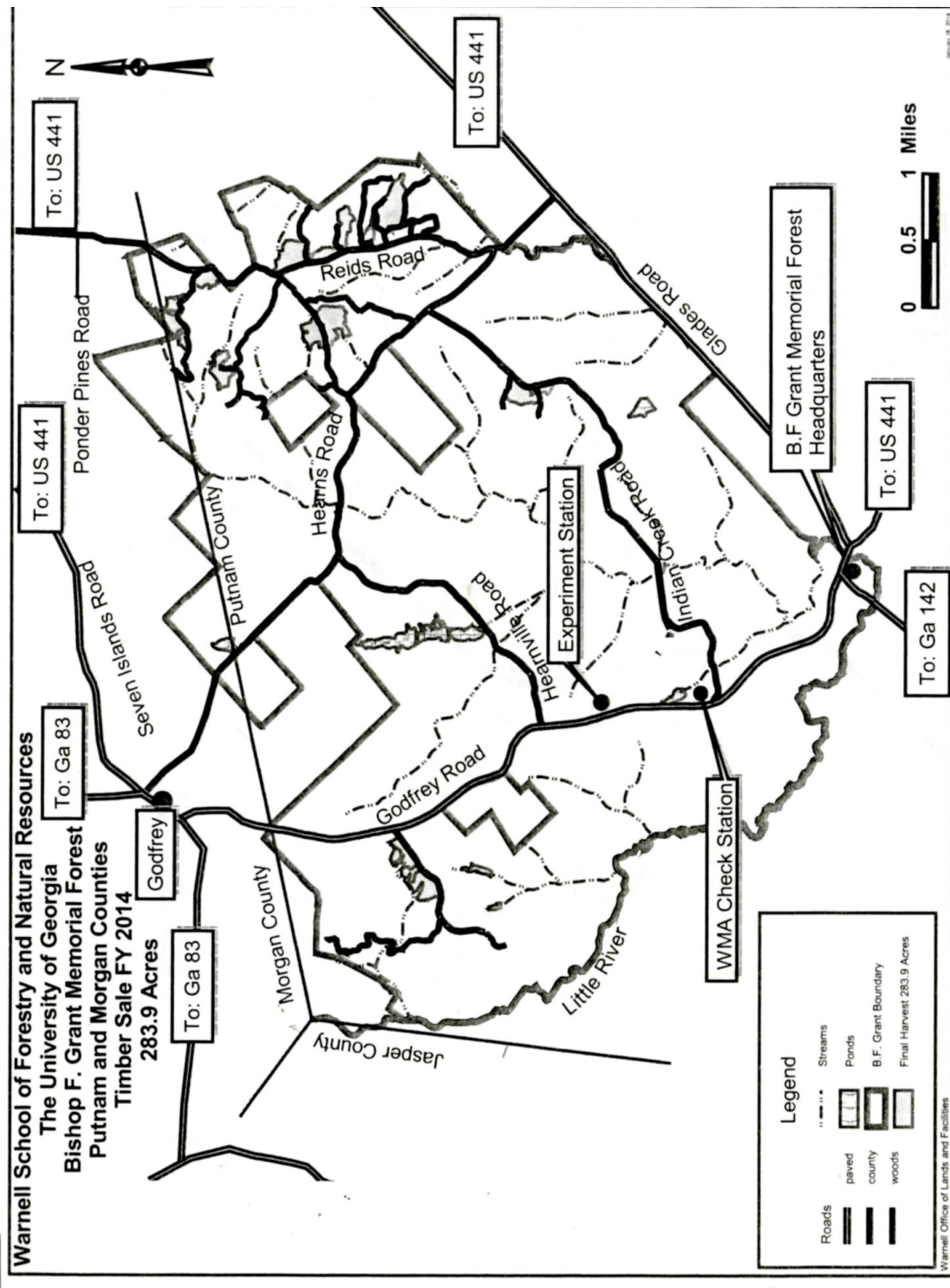


Figure 1.2: Map of the B.F. Grant Forest, (Source: D. B. Warnell School of Forestry and Natural Resources, University of Georgia, Athens, GA. Unpublished)

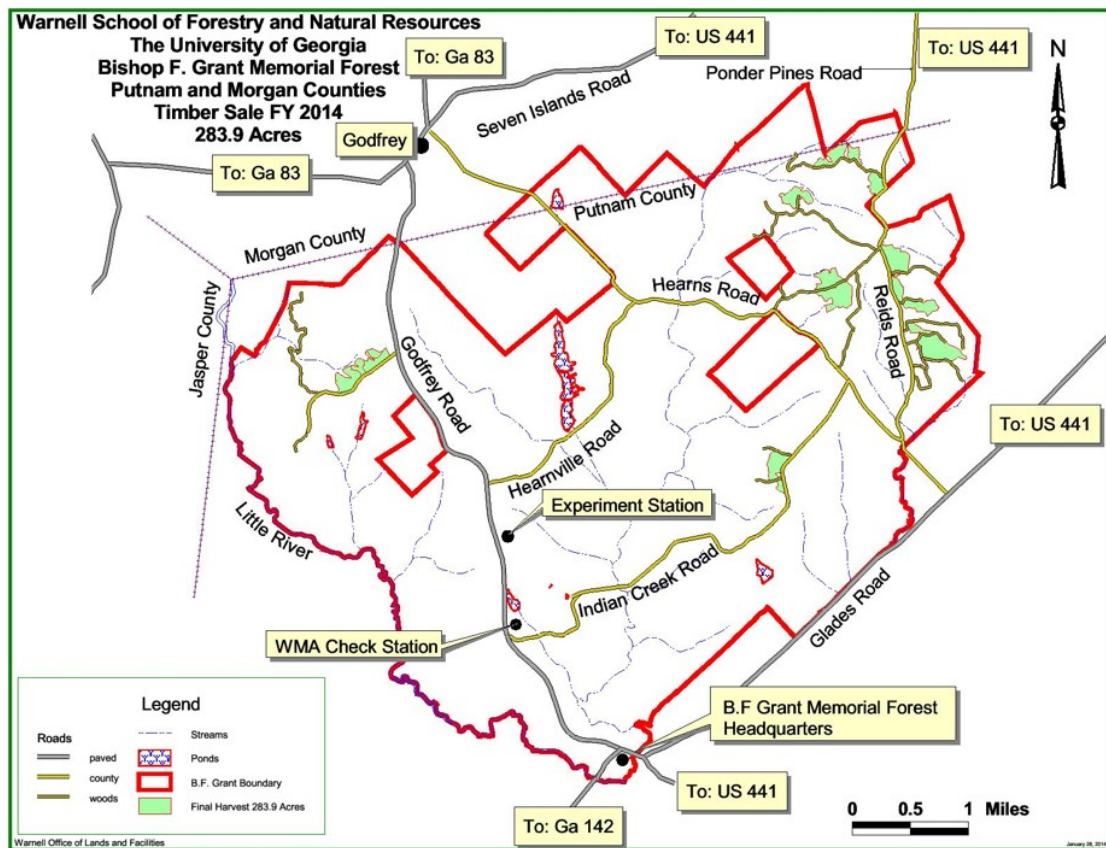


Figure 1.3: 2014 Timber sale map-B.F. Grant Forest, (Source: D. B. Warnell School of Forestry and Natural Resources, University of Georgia, Athens, GA. Unpublished)

CHAPTER 2

LITERATURE REVIEW

The forest inventory and analysis programs estimate and analyze forestry ecosystems and their components. Amongst others, these analyses include the estimation of the coarse woody debris. Coarse woody debris estimation is useful for various aspects like wildlife, forest fire, and carbon modeling sciences. Down woody debris creates many wildlife habitats, for example a dead log is habitat for salamanders in the forest. The estimation of down woody debris is categorized by sizes and helps the fire scientists to calculate the fuel by estimating the fuel hour system. Quantifying the carbon also aids in understanding the effects of climate change [7]. Woody debris residues from timber harvesting available for biomass are generally poorly estimated because the cost value of the timber collection process and transportation is more important when compared with the value of the residues [6]. One of the traditional and common methods of calculating the biomass volume of woody debris is the line intersect sampling (LIS) method or manual plot measurement method. Before the line intersect sampling method, each piece of the woody debris was measured in the defined areas to calculate the volume of the woody debris biomass. In the line intersect method the down wood is sampled along the line transects in the plot. A line intersect method can be applicable for calculating the volume of an entire plot. This method is also used to find the distribution of material in the plot [7]. In this method the wood along the transect is collected, their length and diameter measured, and applied in the formula:

$$T = (1.2337/L) \times \sum_{i=1}^n d_i^2 \quad (2.1)$$

where,

T is the cubic volume of downed woody debris (m³/hectare)

L is the total length of transect (m)

d_i is a diameter of i^{th} intercepted piece (cm)

n is the number of woody debris ¹

The quality of estimating line intersect sampling (LIS) methods increases when the targeted area or down woody debris plot is large in size [15]. Manual plot measurement involves the volume calculation of the woods pieces that were collected from the subplots of the particular plots. Here, only the woody material above 4 cm in diameter is considered. The length and diameter of each piece in the subplot are measured manually and applied in the calculation of cubic volume of downed woody debris. The accuracy of volume estimates using the LIS method increases with increasing total transect length [13] [26]. In another study [21] an 8 ha area with nineteen 30 m transects, or roughly 70 m of transect per ha was worked by two men in 5 hours, taking 680 individual debris measurements. The laser rangefinder is considered to be a better method of calculating the volume of the woody debris than the traditional method [6]. Estimating the volume of biomass of coarse woody debris using recent techniques are discussed below.

2.1 USE OF LIDAR IN ESTIMATING VOLUME OF BIOMASS OF COARSE WOODY DEBRIS

Lidar is an emerging technique in remote sensing to study the earth surface. Lidar data are collected from aircrafts by sending and receiving pulsed laser beams to construct the 3D point model of the earth surface. Lidar can precisely model the earth surface, which plays a vital role in the decision making process of forestry management.

Lidar can be used to describe vegetation structure and aid in assessment of timber management, wildlife habitat, forest health management and deriving potential biofuel availability information [11]. Lidar has been used to estimate the volume of the forest and its biomass [16]. It can be used to identify tree crowns and to construct a 3D model of the forest, which helps to identify the residues on the ground to estimate the biomass. Estimation of the volume of trees has been

¹Derived from Van Wagner's (1968) original equation

accomplished by segmenting the crown area and individual tree. The diameter of the stems have also been calculated from the individual trees [3].

Lidar data also aid in identifying the large woody debris on the beaches. Lidar data can be used to discriminate between features that typically have similar spectral reflectance and are difficult to distinguish from imagery alone such as the difference between the beach sands and large woody debris [1]. This classification is needed to calculate the volume of the large woody debris on the beaches. Also, Lidar data are considered to be an accurate data source for volume, when compared with the field volume based geometric equation method (EEP) for calculating the volume of pile of woods [19].

Because airborne Lidar data are expensive to collect and may not be readily available, alternative methods for creating a 3D point cloud are needed. Image based photogrammetry, often called structure from motion, can be used to create 3D point clouds and derive DSMs from multi-image matching [4]. A UAS can capture the aerial images for photogrammetric analysis more quickly than planes and helicopters and is relatively inexpensive. Certain UAS systems can register the spatial positions of photos when capturing the images. Software such as Photoscan (Agisoft LLC) and Quick Terrain Modeler (Applied Imagery) can align the images by matching points in multiple images with approximately 90% overlap, and form a 3D model. Like aerial photography, UAS captured aerial imagery helps to differentiate landscape features. Similarly some basic steps of aerial photography should be followed in the flight plan for acquiring UAS imagery as well as laying out ground control points before images are flown.

2.1.1 GROUND CONTROL POINTS

Ground control points are physical substances (plywood or heavy cloth) in the ground whose coordinates are known. This helps in determining the position and angular orientation of the aerial imagery at the instant of exposure and also helps to georeference the aerial imagery. Ground control points must be positioned in a flat area and be visibly clear on both ground and imagery. On

the ground survey, control points can be established with coordinates of their position. GPS coordinates of the ground control points must be measured since they will be the only known reference between the ground and aerial imagery. Prior to UAS image capture, control points are marked with contrast to the background located in the ground with crosses on contrasting plywood or heavy cloth [5].

2.1.2 FLIGHT PLANNING

Flight planning depends on several factors such as weather, GPS signals from a certain number of satellites and the obstacles. Flight planning influences time and expense to acquire aerial photos. Flight planning for UAS to capture aerial imagery involves [5]:

1. Determination of the flying height of the UAS
2. Number of flight lines to cover the targeted area
3. Speed of the UAS
4. Time intervals between each exposures.
5. Selecting the time of day and weather for best sun illumination, cloud-free and low wind conditions.

2.1.3 UAS AERIAL PHOTOGRAPH

Vertical aerial photographs are traditionally taken along flight lines to capture all the objects in the targeted field. Successive photos are taken with endlap and sidelap (Figure 2.1) to cover the entire area of the targeted area. Overlapping vertical photographs along flight lines with at least 100% forward overlap are needed to form stereopairs. The height and speed of the flight determines the overlap coverage [5]. In this method using a UAS for 3D point cloud formation, a combination of vertical and oblique (side looking) images should be flown. This ensures common points are visible on multiple (atleast 6) images. Also, frames of 80 to 90% overlap are desired and can be extracted from video acquired from the UAS camera.

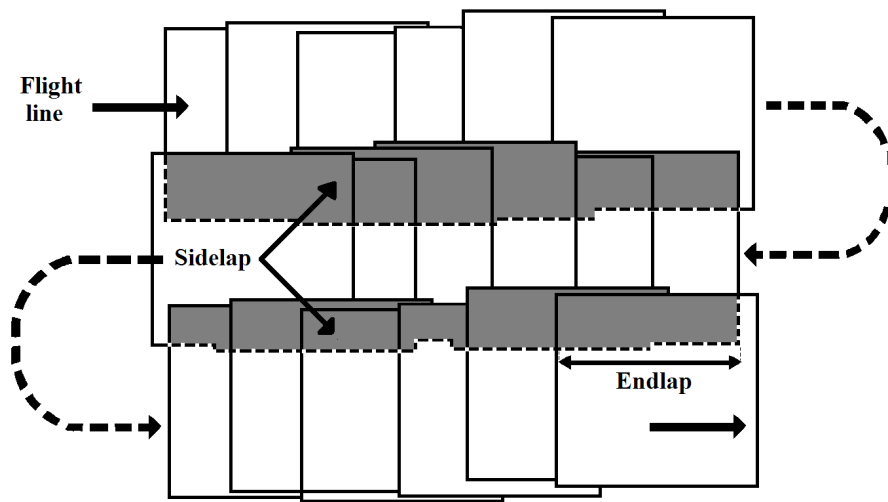


Figure 2.1: Flight path to capture vertical aerial photograph [5]

Application of UAS for precision agriculture is noteworthy because using different sensors like high resolution RGB cameras, multispectral and hyperspectral cameras, thermal infrared and Lidar sensors as payload in the UAS provide a variety of remotely sensed spatial coverage. High resolution satellite imagery has been used to understand the variations of crops and soils, but low altitude remote sensing considered to be an alternative [27]. For example, the Green Area Index (GAI) can be estimated from low altitude RGB imagery and used in decision making process of wheat and rapeseed crops [22]. Here, a UAS was mounted with four cameras for sensing in the green, red, blue and infrared portions of the spectrum to capture multispectral images [22]. Similarly, UAS have made monitoring the field and inventory assessment relatively accessible for individuals at low cost on the order of 2000 USD. The UAS imagery can be input to photogrammetric software to perform structure from motion analysis to reconstruct the 3D structure of objects and landscapes.

2.2 STRUCTURE FROM MOTION

Structure from motion is the construction of 3D models from a series of overlapped images which provide multiple perspectives of the object. The structure from motion (SfM) technique identifies the geometry and position of the object automatically by matching the features from different images taken from different angles, whereas traditional methods need the position of the camera and 3D location of the objects [25]. Since structure from motion is a low cost and fast technique to construct 3D point clouds and models, there is considerable interest and rapid growth in using it in geoscience applications.

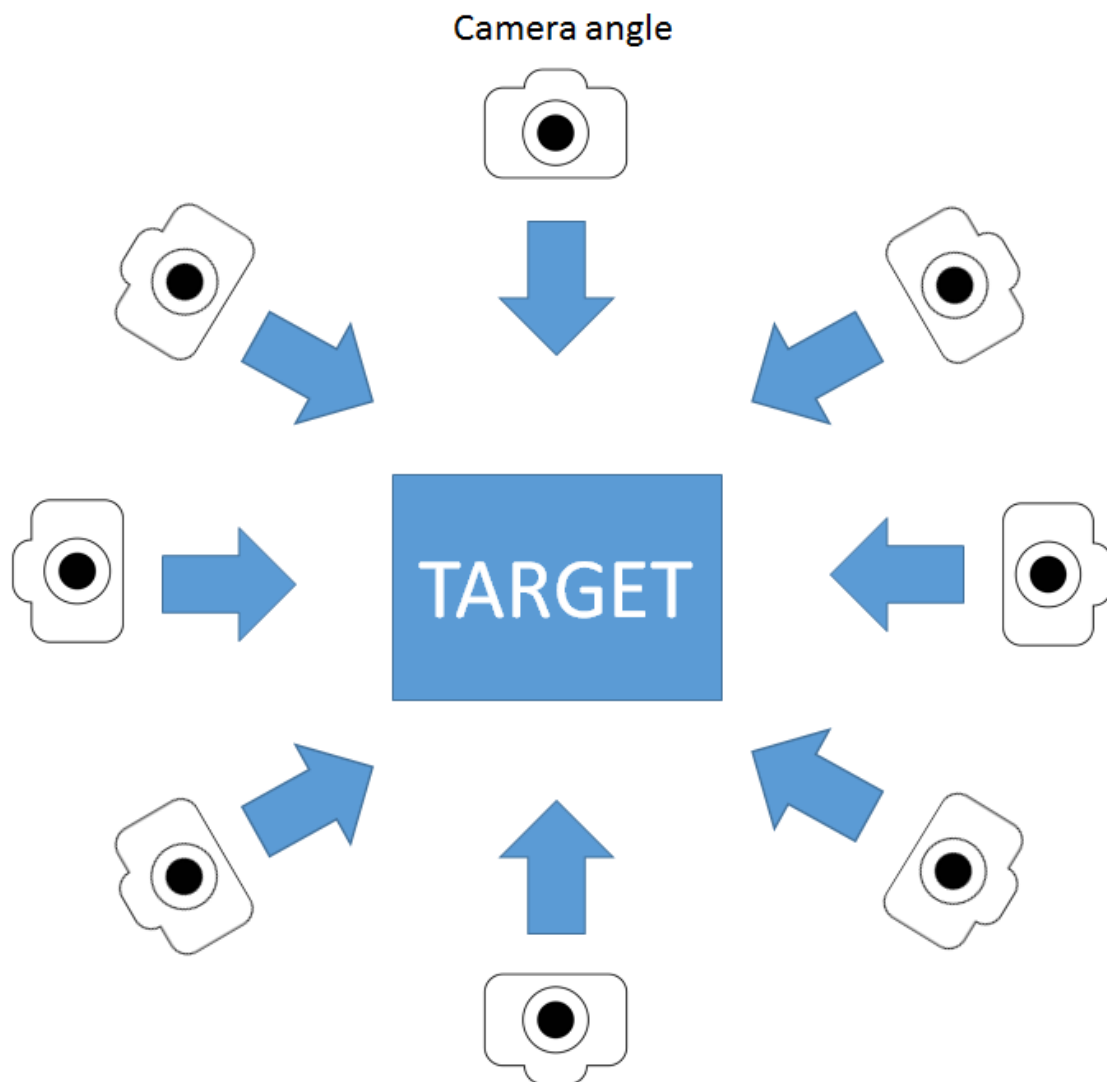


Figure 2.2: Input images used to construct 3D model- structure from motion [25]

CHAPTER 3

MATERIALS AND METHODS

3.1 FIRST TEST SITES

First test sites were located in the University of Georgia B.F. Grant Forest near Eatonton, Georgia. Four 0.25 ha (50 m x 50 m) plots, two at each of the two locations (Godfrey road and Indian Creek Road) (Figure 3.1, 3.2) on the forest, were established in favor of flying the UAS to capture the aerial imagery. The selected areas corners were marked with rebar and perimeters were marked with flags 10 m apart. The two subplots were established within the selected plots in two different sizes, mini-plots 10 m x 10 m and micro-plots 5 m x 5 m. The subplots were located on the edges and sides of the plots. The GPS locations of the corners and centers of plots were noted. Ground control points (GCPs) were made with white painted plywood (0.6 m x 0.6 m) marked with a cross to indicate the center using black duct tape. A hole in the center of the each target positioned it over the rebar.

3.2 SECOND TEST SITE

A second test site was located in the University of Georgia Whitehall Forest, Athens, Georgia. The site was selected to validate volume calculated with the UAS-derived 3D point cloud using a target of known volume, four paper boxes. Conditions were ideal for this test, namely, the field was flat, there were no piles of wood, no debris, or trees in the field. Seven GCPs were placed in the flat surface field for georeferencing the UAS imagery, along with a target of four paper boxes taped together to make a rectangular object of dimensions 72 inches length, 11.5 inches breadth and 9 inches height. The GPS coordinates of the location of all the GCPs were noted.

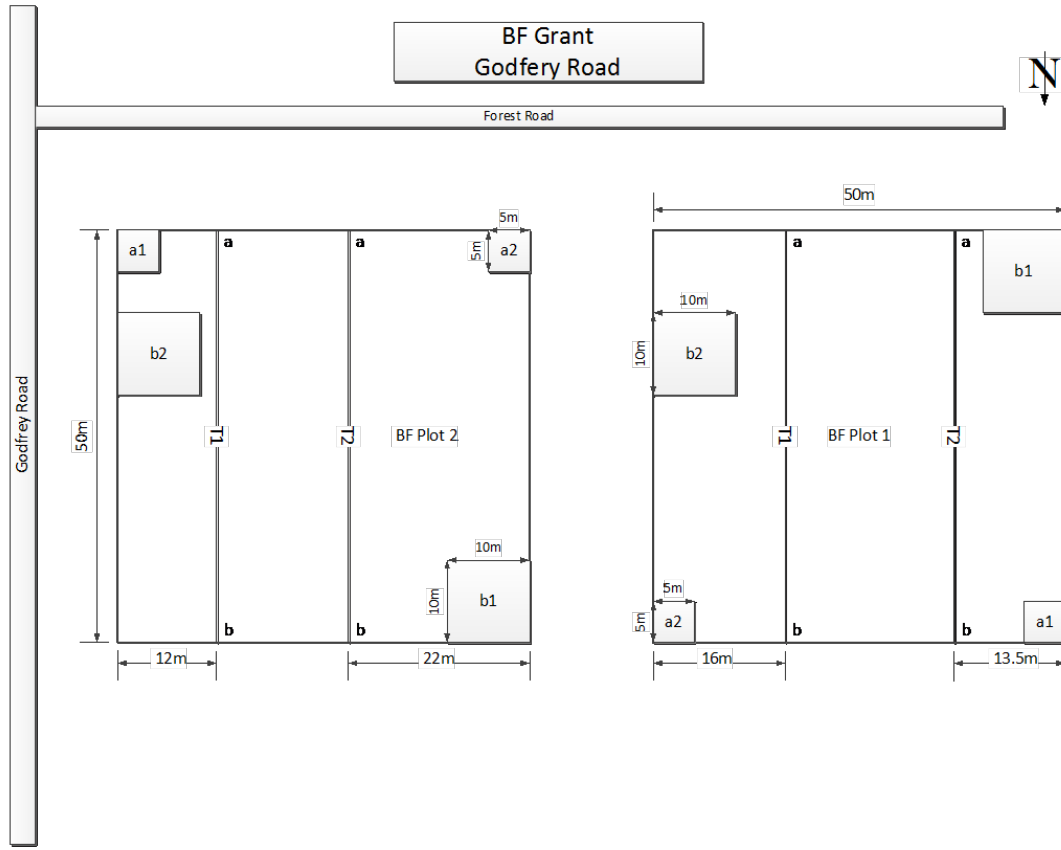


Figure 3.1: Location of plots and transects within each of four 0.25 ha plots at the B.F. Grant Forest, Source: Chris Warren, D. B. Warnell School of Forestry and Natural Resources, University of Georgia, Athens, GA.

3.3 UAS FLIGHTS

Flights of the UAS were conducted on February 11, 2015, in test site 1 with calm winds and clear sky. Before flying the UAS, the GPS coordinates for all corners and centers of every main plot were rechecked using a Trimble Geo H mapping grade GPS receiver. A UAS (DJI Phantom 2 Vision Plus quadcopter) (Figure 3.4) was flown at 25 m to 30 m altitude above the ground along a standard flight path to collect the video of each plot (Figure 3.5). The UAS camera collected video in 14-megapixels/1080p resolution. All the four flights were conducted between 10:30 am

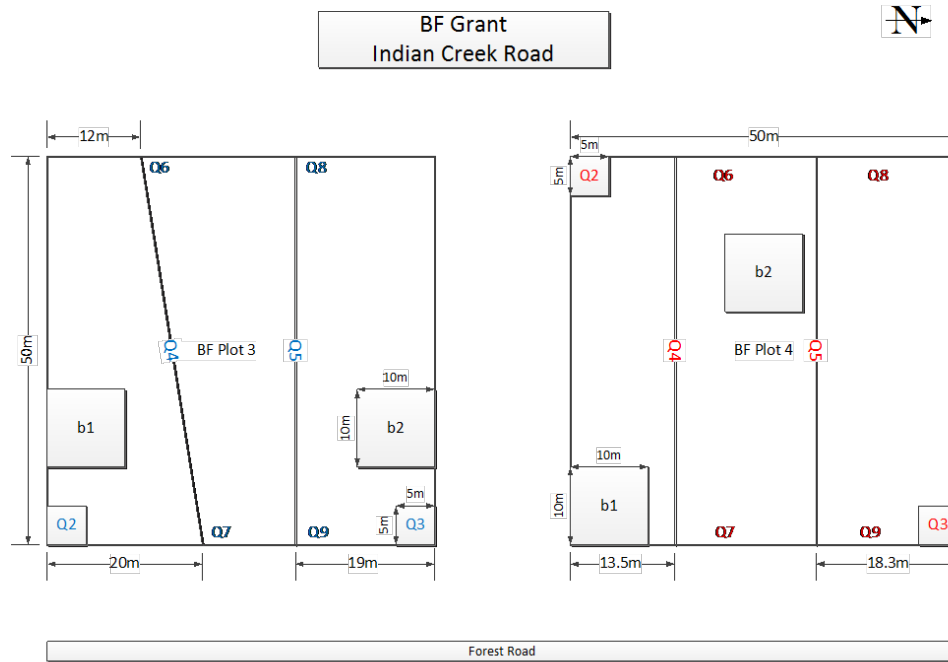


Figure 3.2: Location of plots and transects within each of four 0.25 ha plots at the B.F. Grant Forest, Source: Chris Warren, D. B. Warnell School of Forestry and Natural Resources, University of Georgia, Athens, GA.

and 1:30 pm. Each flight it takes approximately 15 minutes to complete. On October 14, 2015, similar UAS flight procedures were followed to capture the aerial imagery of the second test site.

3.4 FIELD ESTIMATES OF CWD VOLUME

Field measurements were started immediately after the UAS flights over a period of six-weeks, but before the onset of spring growth of vegetation. Calipers, meter sticks, and measuring tapes were used to calculate the diameters of each CWD piece of 4 cm diameter or larger that intersected the line transects. The length and diameter of every CWD piece in the mini (10 m x 10 m) and micro- plots (5 m x 5 m) were measured and recorded. After drawing the plot maps, the CWD



Figure 3.3: Aerial view of Test Site 2 containing ground control points and target of known volume in Whitehall Forest.

volumes were calculated from the field measurements for each transect using (see Eq. 2.1). The CWD volume of the subplots was estimated using the volume of a cylinder equation. A total area of 250 m^2 was measured on every plot following the addition of two $10 \text{ m} \times 10 \text{ m}$ mini-plots to each. This was a 10% sample of each plot and a total of 10% sampling of 1 ha cumulative areas of plots. Totally, it took two people 90-120 mins to sample each $10 \text{ m} \times 10 \text{ m}$ mini-plot depending upon the CWD on each plot. We measured along two 50 m transects on each of four 0.25 ha plots, or 400 meter per hectare, which is more extensive and intensive.



Figure 3.4: Unmanned Aerial System(UAS)(DJI Phantom 2 Vision Plus quadcopter)

3.5 AERIAL ESTIMATIONS OF CWD VOLUME

Aerial estimations of residual biomass were completed in four steps (Figure 3.6): video image capture by UAS, photo frame capture and selection from video, photogrammetric point cloud development using Photoscan, and volume estimation with Quick Terrain Modeler. A VLC media player was utilized to save full resolution screen captures from the video at two-second intervals. Approximately 130 photos having 80-90% were captured for each 50 m x 50 m plot.

The Photoscan workflow was completed as follows:

1. Add photos

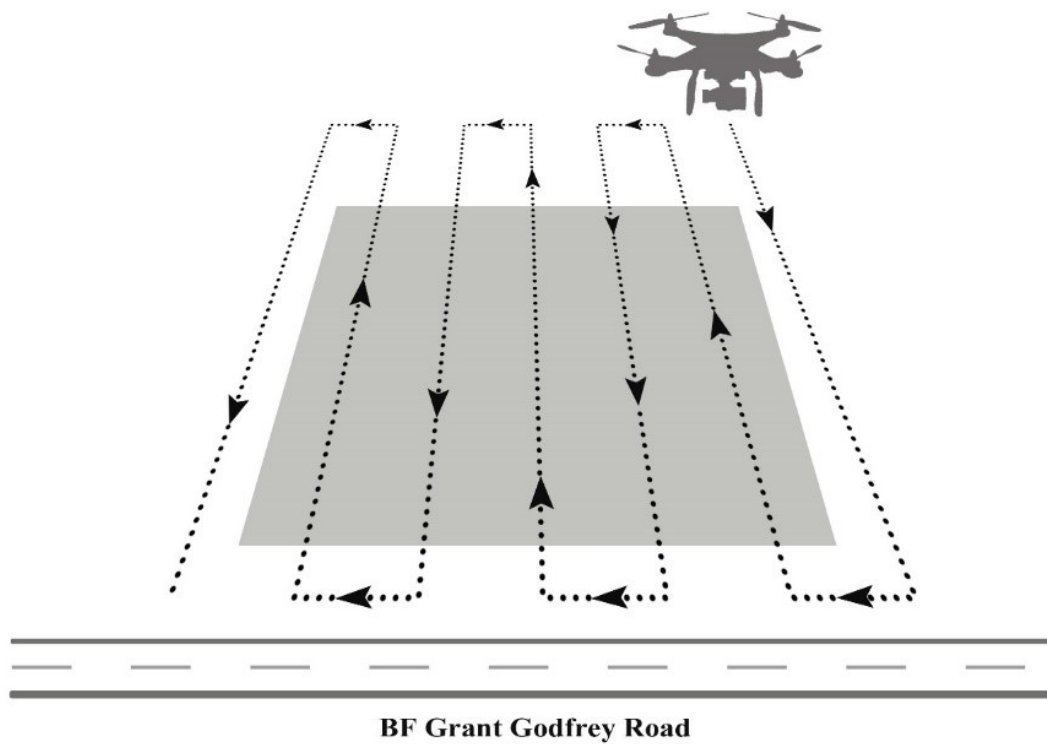


Figure 3.5: Example of a standard flight path flown by the quadcopter to capture video images of 50 m x 50 m plots

2. Align the photos, Photoscan searches the common points on multiple images and also finds the camera position to define the sparse cloud point model. (Note: Some photos cannot be aligned automatically but were aligned manually).
3. Build dense point cloud. Photoscan develops the dense 3D point cloud model according to the target quality setting in this step. Here Photoscan finds the points from the images at large scale. These points are represented in three dimensional coordinates (X, Y, Z) (Figure 3.6).
4. Build a mesh. Edit the 3D model if there are any holes or corrections needed in the mesh.
5. Incorporate texture to the 3D model.

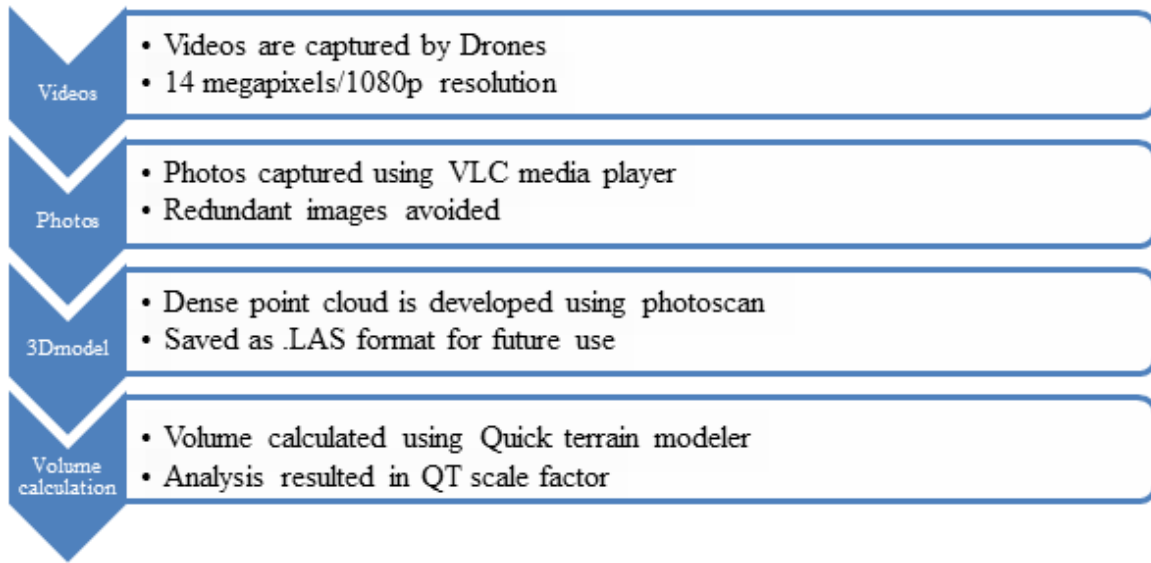


Figure 3.6: Overview of steps used for aerial estimation of woody biomass volume.

Photoscan develops the point dense cloud by identifying the x, y, and z coordinates of each point identified on multiple images taken from different perspectives or angles.

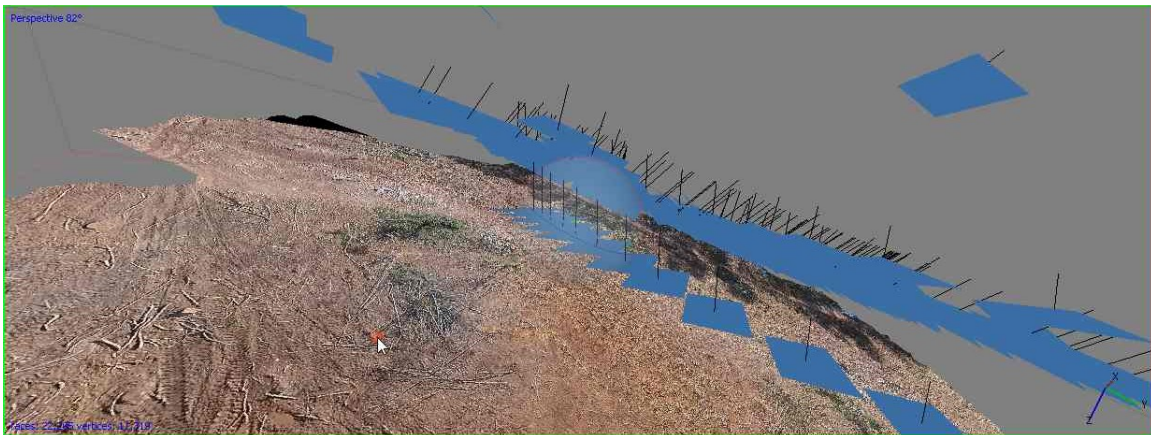


Figure 3.7: 3D model of Plot 1 created using Photoscan. (Blue flags represent the image angles and images used to developed the 3D model).

The Quick Terrain Modeler (QTM) workflow was completed as follows (Figure 3.8):

1. Input .LAS format of point dense cloud.

2. Use GCPs location points (GPS in field) to create a point dense cloud in Photoscan that is georeferenced and scaled to meters.
3. Plots are marked using place markers in Photoscan.
4. A digital elevation model (DEM) is generated for the ground surface using 50 points selected from the georeferenced point cloud that are clearly visible on the soil. Latitude (Y), longitude (X), height (Z), and R, G, B of points are included in the data set. Inverse distance weighted (IDW) interpolation algorithm is used to develop DEM from point cloud data in ArcGIS.
5. Digital surface model (DSM) is developed from dense point cloud as raster data in ArcGIS to match DEM and the difference between the two models is computed for marked (masked) plots.

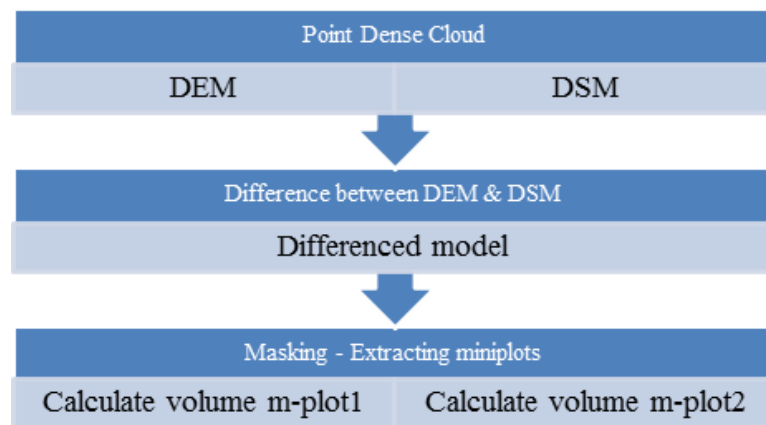


Figure 3.8: Overview of the volume calculation algorithm

3.6 DIGITAL ELEVATION MODEL

Randomly 60 to 70 points were extracted from each 3D point cloud model of plots. Each extracted point consists of X, Y and Z values of the location i.e. longitude, latitude and height respectively. The IDW (Inverse distance weighted) tool in ArcGIS was used to develop a digital elevation model (DEM) by a linearly weighted combination of the extracted points from the 3D point model of the plots and the interpolated surface.



Figure 3.9: Digital Elevation Model of Plot 1

3.7 DIGITAL SURFACE MODEL

The Triangular Irregular Networks (TIN) tool in ArcGIS was used to develop a digital surface model (DSM). The TIN data model connects points to form triangles with Delaunay triangulation which ensures there are no points inside another triangle, the edges are contiguous and there are no overlapping triangles. The TIN to raster conversion algorithm was used to create the DSM.

3.8 DIFFERENCE OF DEM AND DSM OF PLOT 1

The resulted DEM and DSM were subtracted to determine the volume of coarse woody debris on the surface. Later, the subplots were clipped from the difference model and their volumes were identified.

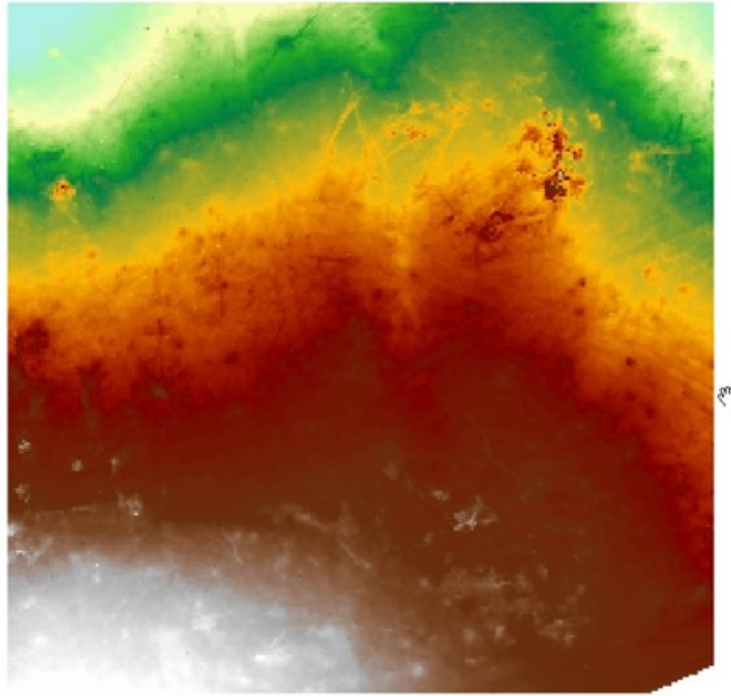


Figure 3.10: Digital Surface Model of Plot 1

CLIPPING

There were two mini subplots (10 m x 10 m) in every main plot. By knowing the location of the mini subplots, DEM-DSM difference plots could be clipped by using the clipping tool in ArcGIS. The resulting model is represented in Figure 3.12.

The volume of the clipped DEM-DSM subplots were higher than the manual calculation derived from the line intersect method. In further analysis we determined that large logs, dead trees and bushes were calculated in the volume of the clipped subplots there by adding volume of objects beyond those measured manually in the field (over estimation of volume). We removed those materials for which volume measurements were desired by identifying them using conditional statements in ArcGIS. Conditional statements were set to differentiate the woody debris residues and big logs according to the coded height difference.

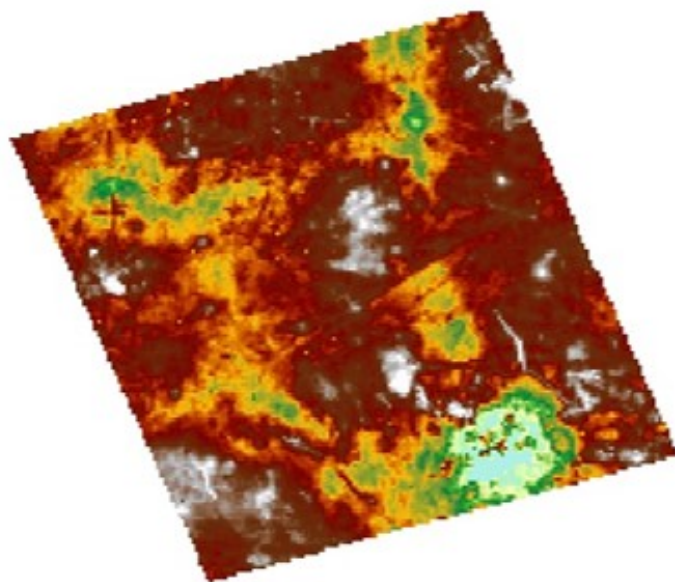


Figure 3.11: Difference of DEM and DSM of Plot 1

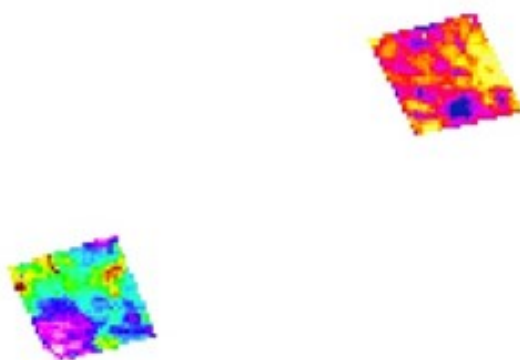


Figure 3.12: Sub plots of Plot 1

CHAPTER 4

RESULTS AND DISCUSSION

4.1 WOODY DEBRIS VOLUME ESTIMATION

The CWD volumes for each plot estimated from field measurements are shown in Tables 4.1-4.4. It could be shown that harvested sites with a heterogeneous distribution of debris can lead to a large degree of variability in measured volumes of CWD derived from UAS-3D point cloud vs field measurements. Our results indicate a variability of over 100% between transects on the same plot, and an even greater variability for measurements made on the small subplots. The uneven spatial distribution of residues in the field is to be considered as the contributing factor for this inconsistency. For example, many piles of woody debris that were in the 50 x 50 m image (Figure 4.1) were not included.

The DEM-DSM difference approach based on image analysis and point clouds was developed and applied to all four (50 m x 50 m) B.F. Grant Forest UAS research test plots. The analyses for the mini-plots are included in Tables 4.1-4.4. The coarse woody debris volume estimates for the test plots are presented. In regard to the volume estimation, there is a poor correlation between 3D images and field measurement estimates; and the variance did not follow a general trend or pattern which suggested that the variation was not from a scalar issue. For the larger 50 m x 50 m plots, estimates of volume (m^3/ha) from the 3D images were unreasonably greater in magnitude than the field measurement estimates and have been disregarded. A possible explanation for the high deviation in volume estimates from both measurements is the algorithm used in the DEM-DSM differencing; the DSM interpolation program could be creating a more generalized and smooth surface instead of displaying the roughness of the residues.

Table 4.1: Plot 1 off the Godfrey Road

| Type | Size (m) | 3D Image | | Field Measurement | |
|---------------|-------------|--|---|--|--------------------------------------|
| | | Vol. Plot basis (cm ³ /plot) | Vol. ha basis (m ³ /plot) | Vol. Plot basis (cm ³ /plot) | Vol. ha basis(m ³ /ha) |
| T1 | 50 long | | 2243.5 | | 108.06 |
| T2 | 50 long | | | | 68.80 |
| Mini-plot | 10 x 10 | 206,120 | 20.61 | 226,563 | 22.66 |
| Mini-plot | 10 x 10 | 162,602 | 16.26 | 711,381 | 71.14 |
| Mean | | | | | 58.27 |
| Std Deviation | | | | | 31.76 |

Table 4.2: Plot 2 off the Godfrey Road

| Type | Size (m) | 3D Image | | Field Measurement | |
|---------------|-------------|--|---|--|--------------------------------------|
| | | Vol. Plot basis (cm ³ /plot) | Vol. ha basis (m ³ /plot) | Vol. Plot basis (cm ³ /plot) | Vol. ha basis(m ³ /ha) |
| T1 | 50 long | | 1411.3 | | 114.13 |
| T2 | 50 long | | | | 31.41 |
| Mini-plot | 10 x 10 | 406,968 | 40.70 | 367,295 | 36.73 |
| Mini-plot | 10 x 10 | 194,709 | 19.47 | 397,061 | 39.71 |
| Mean | | | | | 60.09 |
| Std Deviation | | | | | 31.55 |

Table 4.3: Plot 3 along Indian Trail Road

| Type | Size (m) | 3D Image | | Field Measurement | |
|---------------|-------------|--|---|--|--------------------------------------|
| | | Vol. Plot basis (cm ³ /plot) | Vol. ha basis (m ³ /plot) | Vol. Plot basis (cm ³ /plot) | Vol. ha basis(m ³ /ha) |
| T1 | 50 long | | 1901.5 | | 85.39 |
| T2 | 50 long | | | | 74.59 |
| Mini-plot | 10 x 10 | 421,756 | 42.17 | 292,631 | 29.26 |
| Mini-plot | 10 x 10 | 482,046 | 48.20 | 593,072 | 59.31 |
| Mean | | | | | 62.18 |
| Std Deviation | | | | | 29.87 |

Table 4.4: Plot 4 along Indian Trail Road

| Type | Size (m) | 3D Image | | Field Measurement | |
|---------------|-------------|--|---|--|--------------------------------------|
| | | Vol. Plot basis (cm ³ /plot) | Vol. ha basis (m ³ /plot) | Vol. Plot basis (cm ³ /plot) | Vol. ha basis(m ³ /ha) |
| T1 | 50 long | | 3264.8 | | 23.44 |
| T2 | 50 long | | | | 54.4 |
| Mini-plot | 10 x 10 | 368,464 | 36.84 | 732,523 | 73.25 |
| Mini-plot | 10 x 10 | 333,810 | 33.38 | 297,709 | 29.77 |
| Mean | | | | | 41.76 |
| Std Deviation | | | | | 24.68 |

The results from this first attempt in the new approach indicate that the DEM-based method to post-harvest biomass estimates is viable, but can be implemented operationally only after certain improvements are made. We anticipate that utilizing a multi-faceted method by simultaneously analyzing high-resolution DEM and spectral information captured by aerial sensors will produce great improvement in the separation of surface soil and other weedy ground cover from the downed woody debris.

In order to compare woody debris volume derived from point clouds vs field measurements for a smaller area, the big logs and bushes clipped from the subplots were removed to obtain only coarse woody debris in the difference model. The resulting model appears in (Figure 4.2).

The volume of the mini subplot 1 with no dead trees or big logs was calculated. From the point cloud to be 2.507 cubic meter per subplot (10 m × 10 m) and from field measurements to be 22.67 cubic meter per ha. Although, volume was reduced to 10% variability compared to field measurement calculations. There is still a difference between the manual calculation and 3D point cloud calculation. Hence, to determine if the point cloud method is producing accurate volume measurements, we tested our algorithm with a target of known volume in the field (Test site 2).



Figure 4.1: 3D image with residue piles identified. Volumes associated with these piles were not included in either mini plot or line intersect sampling. They appear to be responsible for differences in volume estimates between field sampling and 3D image sampling.

4.2 TEST SITE 2 RESULTS

The volume of the rectangular target object is,

$$V = L \times W \times H \quad (4.1)$$

where,

V is volume of the rectangular object (four attached paper boxes)

L is the length of the paper boxes

W is the width of the paper boxes

H is the height of the paper boxes

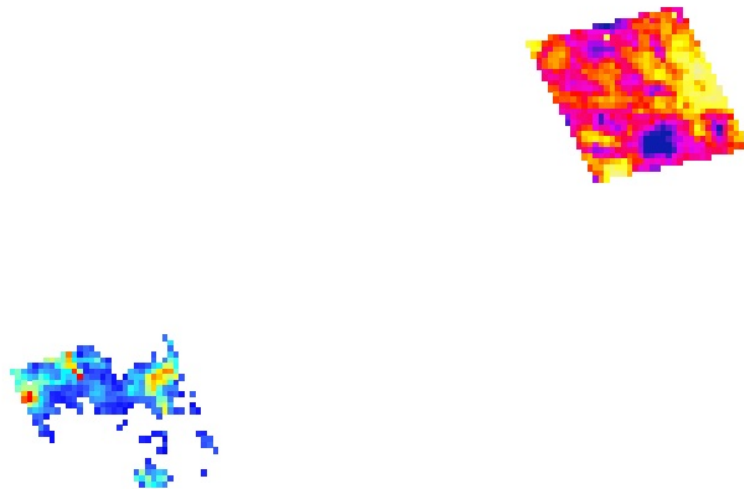


Figure 4.2: Removal of dead trees and bushes

By applying the known target dimensions (measurements of the paper boxes) to the volume of the rectangular object formula, the volume of the known targets were calculated. The same procedure which was used to calculate the volume of the coarse woody debris in the B.F Grant Forest sites was applied to the known targets in the Whitehall Forest (Test site 2) field. The volume of the known target (paper boxes) was calculated.

Thus the algorithm proposed in this project was shown to correctly subtract the DSM and DEM to calculate accurate volumes. The resulting volume from the DEM-DSM method for the target object on the field and the known volume were compared in table 4.5. The difference between the two volume was calculated to be 0.0081 cubic meters (810 cubic centimeters).

Table 4.5: Comparison of the manual and 3D image volume calculation of known target field in (m^3)

| Volume of manual calculation | Volume of 3D point DEM-DSM | Difference |
|------------------------------|----------------------------|------------|
| 0.1221 | 0.1140 | 0.0081 |

For Test site 2, in order to have an unobstructed view of the target boxes, the UAS was used in the field having no tall trees and free of obstacles to facilitate the flight of different perspectives and flying heights. The time consumed to fly the UAS to capture the aerial imagery for each plot was three hours, estimating that volume of the coarse woody debris from the 3D point model was six hours. Cost of the UAS used in this project was \$1000. The software packages Photoscan, Quick Terrain Modeler and ArcGIS were used to develop the 3D model and to estimate the volume of woody debris. This method of estimation is less expensive and time consuming comparing with traditional method where it took 8 weeks to collect and measure the pieces of woody debris intersecting the transect lines.

CHAPTER 5

CONCLUSIONS

This project discussed the use of photogrammetric analysis of unmanned aerial system (UAS) imagery to derive 3D point clouds of the landscape and Geographic Information System (GIS) algorithms to calculate the volume (and therefore biomass) of the coarse woody debris in post-harvest forests that are available for biofuel and wildlife habitat. The algorithms introduced by this research involved the calculation of the woody debris volume from the 3D point shape model by using UAS captured aerial images on two sites, B.F Grant Forest and Whitehall Forest in southeastern Georgia, USA. The results from the first attempt at the B.F Grant Forest reveal that the DEM-DSM method to post-harvest biomass estimates is viable compared to manual field methods that are labor intensive, but needs to be improved in certain aspects in order to be implemented operationally. The large difference in the point cloud calculated and manually determined values for the volume of woody debris may be due to a high degree of roughness on the residue surface and high spatial variability of the debris. Future directions include simultaneously analyzing high-resolution DEM and spectral information captured by aerial sensors to produce an improved resolution i.e. details in the separation of surface soil and other weedy ground cover from the downed woody debris. When the same procedure was applied on an object of known volume placed in a test site 2 at Whitehall Forest, the calculated value of volume from the point cloud algorithm and the manual method were in close agreement. These results demonstrate the promise of using relatively inexpensive and operationally flexible remote sensing methods for detailed image collection in forest applications and the use of photogrammetry to derive 3D point clouds from which terrain surfaces can be modeled and above ground biomass quantified. Such volume data has applications in forest management and conservation.

BIBLIOGRAPHY

- [1] J. B. Eamer and I. J. Walker. Quantifying sand storage capacity of large woody debris on beaches using lidar. *Geomorphology*, 118(1):33–47, 2010.
- [2] C. He, M. Convertino, Z. Feng, and S. Zhang. Using lidar data to measure the 3d green biomass of beijing urban forest in china. *PloS ONE*, 8(10):e75920, 2013.
- [3] J. Hyypä, O. Kelle, M. Lehtikoinen, and M. Inkinen. A segmentation-based method to retrieve stem volume estimates from 3-d tree height models produced by laser scanners. *Geoscience and Remote Sensing, IEEE Transactions on*, 39(5):969–975, 2001.
- [4] M. R. James and S. Robson. Mitigating systematic error in topographic models derived from uav and ground-based image networks. *Earth Surface Processes and Landforms*, 39(10):1413–1420, 2014.
- [5] T. Lillesand, R. W. Kiefer, and J. Chipman. *Remote sensing and image interpretation*. John Wiley & Sons, 2014.
- [6] J. J. Long and K. Boston. An evaluation of alternative measurement techniques for estimating the volume of logging residues. *Forest Science*, 60(1):200–204, 2014.
- [7] A. MacFayden and E. D. Ford. *Advances in ecological research*, volume 15. Academic Press, 1986.
- [8] M. Madden, T. Jordan, S. Bernardes, D. L. Cotten, N. OHare, and A. Pasqua. 10 unmanned aerial systems and structure from motion revolutionize wetlands mapping. *Remote Sensing of Wetlands: Applications and Advances*, page 195, 2015.

- [9] R. E. McRoberts, D. G. Wendt, M. D. Nelson, and M. H. Hansen. Using a land cover classification based on satellite imagery to improve the precision of forest inventory area estimates. *Remote Sensing of Environment*, 81(1):36–44, 2002.
- [10] J. Miller, J. Morgenroth, and C. Gomez. 3d modelling of individual trees using a hand-held camera: Accuracy of height, diameter and volume estimates. *Urban Forestry & Urban Greening*, 14(4):932–940, 2015.
- [11] L. M. Moskal, T. Erdody, A. Kato, J. Richardson, G. Zheng, and D. Briggs. Lidar applications in precision forestry. *Proceedings of Silvilaser*, pages 154–163, 2009.
- [12] S. Nebiker, A. Annen, M. Scherrer, and D. Oesch. A light-weight multispectral sensor for micro uavopportunities for very high resolution airborne remote sensing. *The International Archives of the Photogrammetry, Remote Sensing and Spatial Information sciences*, 37:1193–1200, 2008.
- [13] A. F. L. Nemec, G. Davis, and V. F. Region. *Efficiency of six line intersect sampling designs for estimating volume and density of coarse woody debris*. [Research Section], Vancouver Forest Region, 2002.
- [14] D. P. Paine and J. D. Kiser. *Aerial photography and image interpretation*. John Wiley & Sons, 2012.
- [15] S. G. Pickford and J. W. Hazard. Simulation studies on line intersect sampling of forest residue. *Forest Science*, 24(4):469–483, 1978.
- [16] S. C. Popescu, R. H. Wynne, and R. F. Nelson. Measuring individual tree crown diameter with lidar and assessing its influence on estimating forest volume and biomass. *Canadian Journal of Remote Sensing*, 29(5):564–577, 2003.
- [17] J. Primicerio, S. F. Di Gennaro, E. Fiorillo, L. Genesio, E. Lugato, A. Matese, and F. P. Vaccari. A flexible unmanned aerial vehicle for precision agriculture. *Precision Agriculture*, 13(4):517–523, 2012.

- [18] S. Taylor, M. Veal, T. Grift, T. McDonald, and F. Corley. Precision forestry: operational tactics for today and tomorrow. In *International meeting of the Council on Forest Engineering*, volume 23, 2002.
- [19] J. Trofymow, N. Coops, and D. Hayhurst. Comparison of remote sensing and ground-based methods for determining residue burn pile wood volumes and biomass. *Canadian Journal of Forest Research*, 44(3):182–194, 2013.
- [20] J. A. van Aardt and R. H. Wynne. A multi-resolution approach to forest segmentation as a precursor to estimation of volume and biomass by species. In *Proceedings of the American Society for Photogrammetric Engineering and Remote Sensing Annual Conference*, pages 24–28, 2004.
- [21] C. Van Wagner. The line intersect method in forest fuel sampling. *Forest Science*, 14(1):20–26, 1968.
- [22] A. Verger, N. Vigneau, C. Chéron, J.-M. Gilliot, A. Comar, and F. Baret. Green area index from an unmanned aerial system over wheat and rapeseed crops. *Remote Sensing of Environment*, 152:654–664, 2014.
- [23] S. Von Bueren and I. Yule. Multispectral aerial imaging of pasture quality and biomass using unmanned aerial vehicles (uav). *Accurate and Efficient Use of Nutrients on Farms, Occasional Report*, (26).
- [24] W. Warren and P. Olsen. A line intersect technique for assessing logging waste. *Forest Science*, 10(3):267–276, 1964.
- [25] M. Westoby, J. Brasington, N. Glasser, M. Hambrey, and J. Reynolds. structure-from-motion photogrammetry: A low-cost, effective tool for geoscience applications. *Geomorphology*, 179:300–314, 2012.
- [26] G. Woldendorp, R. Keenan, S. Barry, and R. Spencer. Analysis of sampling methods for coarse woody debris. *Forest Ecology and Management*, 198(1):133–148, 2004.

- [27] C. Zhang and J. M. Kovacs. The application of small unmanned aerial systems for precision agriculture: a review. *Precision Agriculture*, 13(6):693–712, 2012.
- [28] Y. Zhang. Problems in the fusion of commercial high-resolution satellite as well as landsat 7 images and initial solutions. *International Archives of Photogrammetry Remote Sensing and Spatial Information Sciences*, 34(4):587–592, 2002.